The EMBO Journal (2004) 23, 1516–1525 | © 2004 European Molecular Biology Organization | All Rights Reserved 0261-4189/04
www.embojournal.org

THE EMBO JOURNAL

A new sea anemone peptide, APETx2, inhibits ASIC3, a major acid-sensitive channel in sensory neurons

Sylvie Diochot, Anne Baron, Lachlan D Rash, Emmanuel Deval, Pierre Escoubas, Sabine Scarzello, Miguel Salinas and Michel Lazdunski*

Institut de Pharmacologie Moléculaire et Cellulaire, Centre National de la Recherche Scientifique, Institut Paul Hamel, Sophia Antipolis, Valbonne, France

From a systematic screening of animal venoms, we isolated a new toxin (APETx2) from the sea anemone *Anthopleura elegantissima*, which inhibits ASIC3 homomeric channels and ASIC3-containing heteromeric channels both in heterologous expression systems and in primary cultures of rat sensory neurons. APETx2 is a 42 amino-acid peptide crosslinked by three disulfide bridges, with a structural organization similar to that of other sea anemone toxins that inhibit voltage-sensitive Na^+ and K^+ channels. APETx2 reversibly inhibits rat ASIC3 ($IC_{50} = 63$ nM), without any effect on ASIC1a, ASIC1b, and ASIC2a. APETx2 directly inhibits the ASIC3 channel by acting at its external side, and it does not modify the channel unitary conductance. APETx2 also inhibits heteromeric ASIC2b + 3 current ($IC_{50} = 117$ nM), while it has less affinity for ASIC1b + 3 ($IC_{50} = 0.9$ μM), ASIC1a + 3 ($IC_{50} = 2$ μM), and no effect on the ASIC2a + 3 current. The ASIC3-like current in primary cultured sensory neurons is partly and reversibly inhibited by APETx2 with an IC_{50} of 216 nM, probably due to the mixed inhibitions of various co-expressed ASIC3-containing channels.

The EMBO Journal (2004) **23,** 1516–1525. doi:10.1038/sj.emboj.7600177; Published online 25 March 2004
Subject Categories: membranes & transport; neuroscience
Keywords: ASIC3; channel; sea anemone; toxin

Introduction

Acid-sensing ion channels (ASICs) are H^+-gated Na^+-permeable channels formed by the homo- or heteromeric association of six different subunits (Waldmann and Lazdunski, 1998): ASIC1a (Waldmann *et al*, 1997b), ASIC1b (Chen *et al*, 1998), ASIC2a (Price *et al*, 1996; Waldmann *et al*, 1996), ASIC2b (Lingueglia *et al*, 1997), ASIC3 (Waldmann *et al*, 1997a; de Weille *et al*, 1998; Babinski *et al*, 1999), and ASIC4 (Akopian *et al*, 2000; Grunder *et al*, 2000). Only ASIC1a, ASIC1b, ASIC2a, and ASIC3 are functionally activated by extracellular H^+ when expressed alone. ASIC2b can modulate heteromeric ASIC currents by inducing a sustained nonselective cation current following the transient peak (Lingueglia *et al*, 1997; Coscoy *et al*, 1999).

In sensory neurons, ASIC currents have been implicated in pain transduction associated with acidosis in inflamed or ischemic tissues (Reeh and Steen, 1996; Waldmann and Lazdunski, 1998; Benson *et al*, 1999; Kress and Zeilhofer, 1999; Pan *et al*, 1999; Sutherland *et al*, 2001; Voilley *et al*, 2001; Mamet *et al*, 2002; Ugawa *et al*, 2002; Krishtal, 2003), particularly ASIC3, which is mainly expressed in sensory neurons (Waldmann *et al*, 1997a; Voilley *et al*, 2001). Recent studies in knockout mice confirm that ASIC3 plays a major role in high-intensity pain stimuli (Price *et al*, 2001; Chen *et al*, 2002) and in acid-induced hyperalgesia (Sluka *et al*, 2003). An involvement in the mechanosensitivity of large sensory neurons has also been proposed (Xie *et al*, 2002).

Further analysis of the involvement of ASIC3 in the electrical activity of nociceptors requires selective pharmacological tools. To date, the repertoire of active ligands on the ASIC3 channel is limited to amiloride, nonsteroidal anti-inflammatory drugs, and Gd^{3+} (Waldmann *et al*, 1997a; Babinski *et al*, 2000; Voilley *et al*, 2001) that act as inhibitors, and to the mammalian neuropeptides NPFF and NPSF that activate ASIC3 (Askwith *et al*, 2000; Deval *et al*, 2003). However, none of these drugs is absolutely specific for ASIC channels.

In the past 25 years, animal venoms have yielded a great number of toxins that modulate specifically and with high affinity voltage-gated Na^+, K^+, and Ca^{2+} currents (Moczydlowski *et al*, 1988; Norton, 1991; Harvey *et al*, 1994; Uchitel, 1997; Tytgat *et al*, 1999; Escoubas *et al*, 2000b), Ca^{2+}-gated K^+ channels (Hugues *et al*, 1982; Shakkottai *et al*, 2001), and mechano-sensitive K^+ channels (Bode *et al*, 2001). Recently, *Conus* toxins have been shown to target neurotransmitter receptors at sensory synapses (England *et al*, 1998). The only toxin known to affect ASIC channels is Psalmotoxin 1 (PcTx1), a tarantula venom peptide that acts as a potent and specific inhibitor of homomeric ASIC1a channels (Escoubas *et al*, 2000a; Escoubas *et al*, 2003). We report here the identification of APETx2, a novel peptide toxin isolated from sea anemone venom, which selectively inhibits homomeric ASIC3 channels as well as the ASIC1a + 3, ASIC1b + 3, and ASIC2b + 3 heteromers. A physico-chemical characterization of APETx2 is presented, including its disulfide bridge arrangement, and a structural model based on its homology with the K^+ channel sea anemone toxin BDS-I. We show that APETx2 inhibits ASIC3-like currents recorded from rat sensory neurons. APETx2 thus constitutes the first pharmacological tool to analyze the physiological involvement of ASIC3-containing channels in neuronal excitability and pain coding.

*Corresponding author. Institut de Pharmacologie Moléculaire et Cellulaire, Centre National de la Recherche Scientifique, UMR 6097, Institut Paul Hamel, 660, Route des Lucioles, Sophia Antipolis, 06560 Valbonne, France. Tel.: +33 493 957702 or 03; Fax: +33 493 957704; E-mail: ipmc@ipmc.cnrs.fr

Received: 12 December 2003; accepted: 25 February 2004; published online: 25 March 2004

Results

Purification of an ASIC3 inhibitory peptide from Anthopleura elegantissima

In order to find effectors of the ASIC3 channel, a large number of scorpion, bee, spider, snake, and sea anemone venoms (1/1000 dilution) or peptide fractions (0.1 mg/ml) were screened on ASIC3 channels expressed in *Xenopus* oocytes. A peptide fraction from the sea anemone *Anthopleura elegantissima* (Bruhn *et al*, 2001) was found to inhibit more than 80% of the rat ASIC3 current stimulated at pH6. The active peptide was purified to homogeneity by bioassay-guided reversed-phase and cation-exchange chromatography (Supplementary Figure A), and was named APETx2.

Biochemical properties

APETx2 is a basic peptide (pI = 9.59) of 42 amino acids, crosslinked by three disulfide bridges and has a calculated 280 nm molecular absorbance of $\varepsilon_{280} = 11170$. Its full sequence was established by N-terminal Edman degradation, and its measured monoisotopic mass (4557.96 Da) was in perfect accordance with the mass calculated from sequence data (4557.88 Da, accuracy 17.5 ppm), indicating a free C-terminal carboxylic acid. APETx2 displays 64% sequence identity (76% homology) with APETx1 (Diochot *et al*, 2003) (Figure 1A) and only 34% sequence identity (57 and 55% homology, respectively) with the BDS-I and BDS-II toxins from *Anemonia sulcata*, which inhibit the voltage-dependent K^+ (Kv) channel Kv3.4 (Diochot *et al*, 1998). Sequence identity with Na^+ channel activators such as AP-A, AP-B, AP-C, APE1-1, and APE-2 from *Anthopleura* sp (Bruhn *et al*, 2001) is only 25–29% (homology 41–47%). APETx2 does not display any sequence homologies with the ASIC1a inhibitor PcTx1 previously isolated from a tarantula venom (Escoubas *et al*, 2000a).

The determination of disulfide bridges in small peptide toxins is crucial to understand and confirm the three-dimensional structure of the toxins. Partial reduction and cyanylation of APETx2 yielded five components separated by HPLC (Supplementary Figure B). MALDI-TOF MS indicated that peaks 2 and 3 predominantly contained singly reduced/cyanylated isoforms (+52 Da). Based on its sequence homology and conserved cysteine spacing with BDS-I, APETx2 was predicted to have similar disulfide pairing. Figure 1B shows the predicted fragments and calculated masses for each disulfide bond of APETx2 and the masses observed from the cleavage of singly reduced isoforms in HPLC peaks 2 and 3. Following cleavage and full reduction, MALDI-TOF MS analysis revealed that peak 2 contained only one singly reduced isoform with the major ions (m/z 2025.53 and 2097.53), corresponding unambiguously to fragments expected for a Cys20–Cys38 (CysIII–CysVI) bond. Analysis of cleavage fragments from peak 3 suggested the presence of two isoforms of singly reduced toxin. The major ions (m/z 2741.71 and 1475.11) corresponded to cleavages at Cys6 and Cys30 (CysII–CysIV), while peptide 3772.86 indicated the reduction and cleavage of a Cys4–Cys37 (CysI–CysV) bond. See online Supplementary data for more details.

APETx2 has the same disulfide arrangement (CysI–CysV, CysII–CysIV, CysIII–CysVI) as BDS-I, the only toxin with high homology to APETx2 for which the disulfides have been deduced (NMR data) (Driscoll *et al*, 1989b). Alternative disulfide bond pairings observed in other sea anemone toxins (HmK: I–VI, II–IV, III–V), or inhibitor cystine knot (ICK) toxins (I–IV, II–V, III–VI) were not supported by experimental data.

Toxin structure

Examination of the three-dimensional structures of BDS-I, APETx1, and APETx2 reveals that they share very similar

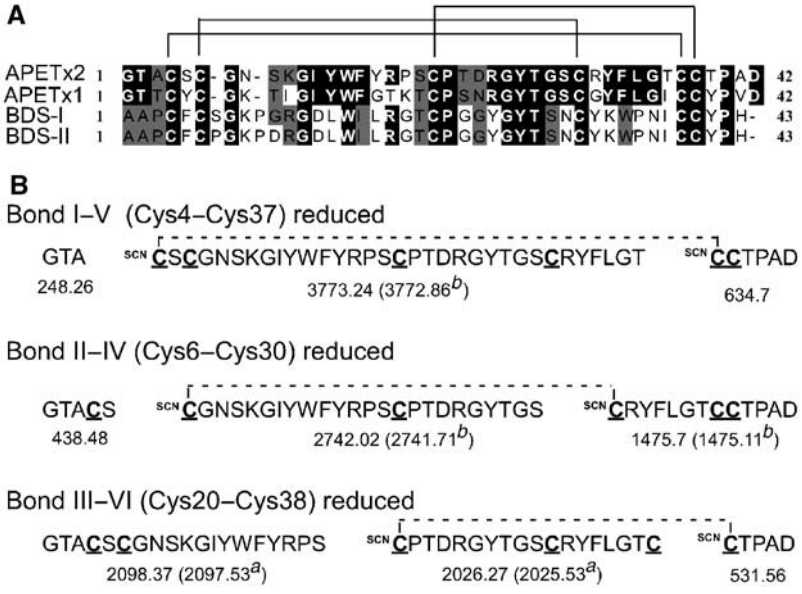

Figure 1 Structural properties of APETx2. (**A**) Sequence alignments of APETx2, with K^+ channel modulators from sea anemones. Black boxes indicate sequence identities and gray boxes sequence homologies with BDS-I and BDS-II (*Anemonia sulcata*), and APETx1 (*Anthopleura elegantissima)*. The three disulfide bonds of APETx2, determined by the partial reduction/cyanylation method, are indicated. (**B**) Expected cleavage fragments of APETx2 and their calculated masses (average mass, M + H +) for singly reduced bonds according to the predicted disulfide bond arrangement. The masses in parenthesis were those observed after cleavage and reduction of peak 2^a and peak 3^b.

features, comprising a triple antiparallel β-sheet motif stabilized by three disulfide bridges. Although the orientation of the N-terminal and connecting loops varies between BDS-I and the APETx toxins, the main differences appear in the surface features. Comparison of BDS-I and APETx1 (Figure 2A, boxed panel) shows that the differences in the primary sequence and therefore amino-acid side chains are primarily reflected on the face of the toxin formed by the N-terminal loop and the last two strands of the β-sheet. APETx1 shows a higher abundance of aromatic residues. Comparison of the differences between APETx1 and APETx2 (Figure 2A) shows that differences in sequence result mostly in surface variations on the opposite side of the toxin and to a lesser extent in the C-terminal area. Of particular significance are the replacements in APETx2 of Tyr5, Lys8, and Ileu10 by Ser5, Asn8, and Lys10, respectively, and the replacement of Gly16, Thr17, and Pro18 by Tyr16, Arg17, and Lys18. The latter induce a tighter turn of the loop connecting the first and second strands of the β-sheets due to Pro18, and comprise a surface that is at the same time bulkier (Tyr16) and bears more positive charges (Figure 2B). The replacement of Gly31 by Arg 31 also contributes to the constitution of a strong basic patch on this side of the toxin. The modifications on the opposite side of the toxin result in a more negatively charged patch, surrounded by an area of hydrophobic or neutral residues. Comparison with BDS-I (Figure 2B) shows that this area is significantly different, and thus may play a role in channel selectivity. The main differences between APETx1 and APETx2 appear to be located on two opposite sides of the molecule, with the β-turn composed of Tyr16, Arg17, and Lys18, which could be hypothesized as a significant selectivity site for recognition of ASIC3.

APETx2 inhibits homomeric ASIC3 current

Rat homomeric ASIC3 currents induced every minute by a rapid step to pH 6 from pH 7.4 were recorded from *Xenopus* oocytes (Figure 3A, ▲) or COS cells (Figure 3A, ●). Toxin-containing solutions at pH 7.4 were perfused before the acidic step. Inhibition of the ASIC3 current started at 10 nM APETx2 and was maximal at 3 μM (Figure 3A and B). The inhibition of ASIC3 currents was rapid and saturated within 30 s of APETx2 perfusion. The concentration–response relationship indicates an IC_{50} of 63 nM (Figure 3A). Effects were totally reversible within 4 min (Figure 3C). The sustained component of ASIC3 current, easily measurable at pH 4, was insensitive to 3 μM APETx2, even though the transient peak component was totally inhibited (Figure 3D).

Human ASIC3 expressed in COS cells was also inhibited by APETx2 with an IC_{50} of 175 nM and n_H of 1 (not shown).

APETx2 (3 μM) perfused for 30 s before the pH drop did not significantly inhibit ASIC1a, ASIC1b, or ASIC2a homomeric currents activated at pH 6 or 5 ($n = 5$–6 cells under each condition, $P > 0.05$, not shown) and expressed in COS cells.

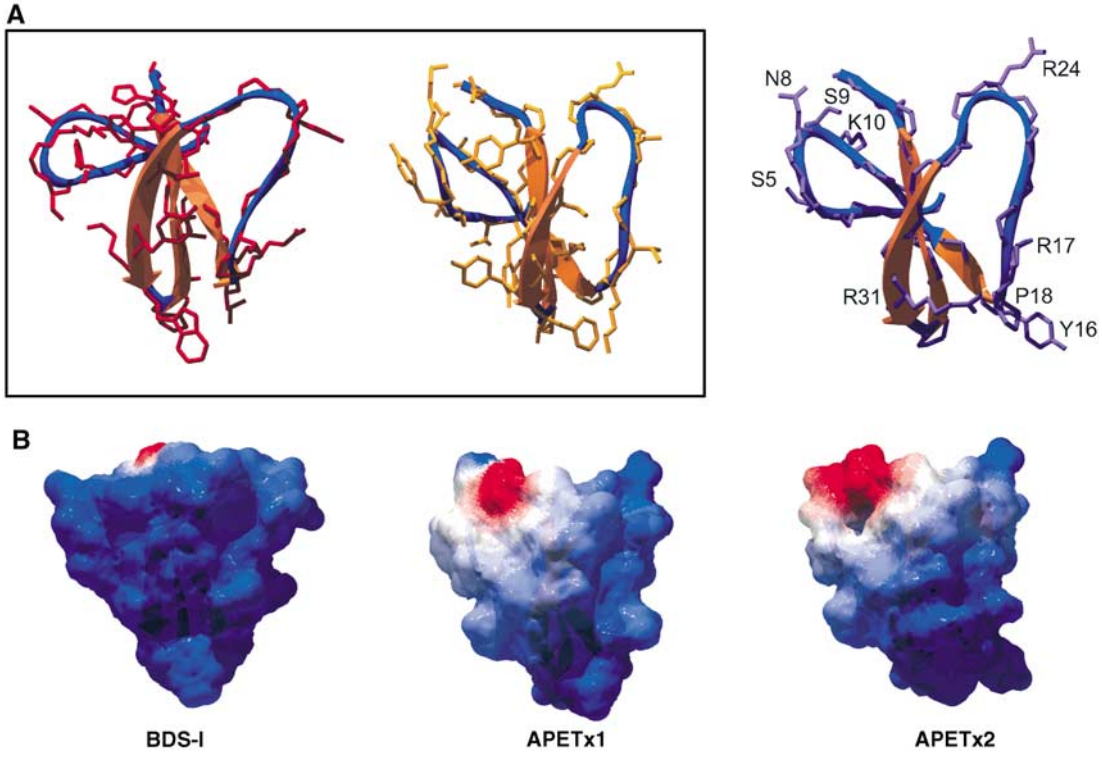

Figure 2 Molecular modeling of APETx2. (**A**) Ribbon representations of BDS-I, APETx1, and APETx2. Peptide backbones and selected side chains are superimposed on the ribbon structure. To compare the models of BDS-I and APETx1 (box), only side chains of nonconserved amino acids are apparent. The model of APETx2 shows side chains differing between APETx1 and APETx2, and Arg24, which could be part of the active site of the toxin. (**B**) Surface representation of the same toxins, mapped with the calculated electrostatic potential distribution (Blue = positive, red = negative, white = neutral) showing the charge distribution on the calculated toxin surface. All structures were generated with DeepView v3.7 and raytraced in PovRay.

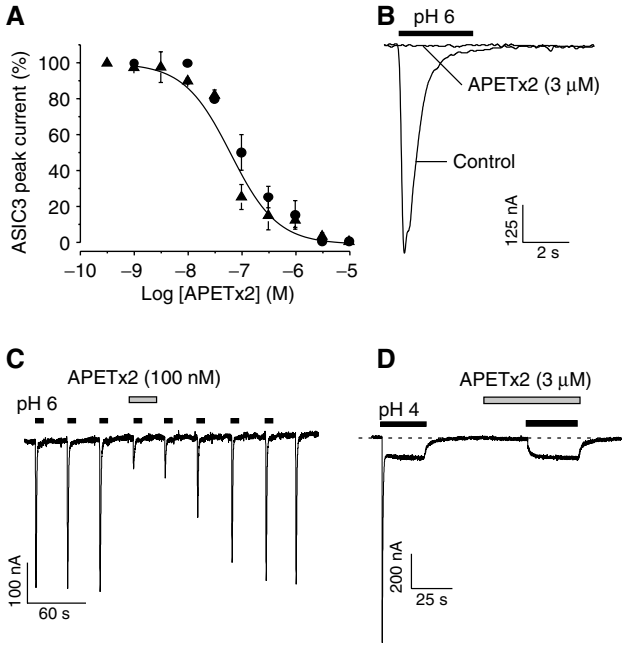

Figure 3 Effect of APETx2 on homomeric ASIC3 current. (**A**) Concentration–response curve for APETx2 effects on ASIC3 channels expressed in *Xenopus* oocytes (▲) and in COS cells (●). Holding potential: −50 mV, pH drop from 7.4 to 6. APETx2 was perfused for 30 s before the pH drop. Data were fitted by the Hill equation ($n_H = 1$) giving an IC_{50} value of 63 nM. Each point is the mean ± s.e.m. (3–6 cells). (**B**) APETx2 (3 μM) totally inhibits the ASIC3 current. (**C**) Effect of 100 nM APETx2 on ASIC3 currents, and reversibility. (**D**) Upon stimulation of ASIC3 at pH4, APETx2 (3 μM) inhibits the peak, but not the plateau phase of the current.

APETx2 directly inhibits homomeric ASIC3 channels in outside-out patches

Unitary ASIC3 currents triggered by an external pH drop from 7.4 to 6.6 were recorded at −50 mV from outside-out patches of transfected COS cells. A high number of channels were usually simultaneously recorded even when submaximally activated at pH 6.6 (Figure 4A). When APETx2 (3 μM) was applied to the bath solution 30 s before the pH drop, it induced a 75 ± 6% ($n = 4$) inhibition of ASIC3 peak current and this effect was rapidly reversible. Amplitude histograms obtained from the analysis of ASIC3 unitary current recorded before (Figure 4Ba) and after (Figure 4Bb) application of APETx2 show that the unitary amplitude of ASIC3 currents was not modified by the toxin. The mean amplitude values are shown in Figure 4C. These results show that the ASIC3 channel is directly inhibited by the toxin, without any change in its unitary conductance. Similar results were obtained with 100 nM APETx2 producing a partial inhibition of the peak outside-out current (58 ± 7%).

Effects of APETx2 on the heteromeric ASIC1a + 3 current

As ASIC1a and ASIC3 channels are co-localized in sensory neurons (Voilley *et al*, 2001; Alvarez de la Rosa *et al*, 2002), we studied the effects of APETx2 on the heteromeric ASIC1a + 3 channel expressed in COS cells using the pBudCE4.1 vector designed for simultaneous expression of two genes under the control of two independent promoters. The current induced at pH 5 exhibits ASIC3-like kinetics and a plateau phase (Figure 5Aa). The inactivation time constant, 258 ± 136 ms ($n = 8$), was comparable to that of the ASIC3 current (440 ± 135 ms, $n = 15$). As shown previously (Escoubas *et al*, 2000a), this current was insensitive to 10 nM PcTx1, a concentration that completely blocks the homomeric ASIC1a current (Figure 5Ab). The ASIC1a + 3 current induced at pH 6 was only partly inhibited (63 ± 10%, $n = 6$) by high concentrations of APETx2 (3 μM). Moreover, the ASIC1a + 3 current appears to be less sensitive than homomeric ASIC3 current, with an IC_{50} of 2 μM ($n_H = 0.9$; Figure 5D, ○).

Effects of APETx2 on the heteromeric ASIC1b + 3 current

The ASIC1b channel is expressed in small- and large-diameter sensory neurons (Chen *et al*, 1998; Alvarez de la Rosa *et al*, 2002; Mamet *et al*, 2002). Co-expression of ASIC1b + 3 subunits in COS cells using the pBudCE4.1 vector resulted in channels carrying a rapidly activating and inactivating current at pH 6, with an inactivation time constant of 346 ± 183 ms ($n = 20$), comparable to that of the ASIC3 current (440 ± 135 ms, $n = 15$, Figure 5C). A plateau phase was recorded at pH 5 and pH 4. Similar to the ASIC1a + 3 current, the ASIC1b + 3 current was inhibited by APETx2, but with a lower affinity than the ASIC3 current ($IC_{50} = 0.9$ μM, $n_H = 0.9$) (Figure 5D, ■).

Effects of APETx2 on the heteromeric ASIC2b + 3 current

Both ASIC2b and ASIC3 are expressed in small- and large-diameter sensory neurons (Lingueglia *et al*, 1997; Voilley *et al*, 2001; Alvarez de la Rosa *et al*, 2002). Their coexpression in heterologous systems results in channels activated at acidic pH with a transient Na^+-selective current, followed by a sustained nonselective cation current (Lingueglia *et al*, 1997). The ASIC2b + 3 sustained current can be recorded as an inward plateau at −50 mV (Figure 5Ba), and as an outward steady-state current at +30 mV and above (Figure 5Bb). Independently of the holding potential, only the peak ASIC2b + 3 current was inhibited by increasing concentrations of APETx2 (Figure 5Ba and b), with an IC_{50} of 117 nM ($n_H = 1$, Figure 5D, ●).

Effects of APETx2 on the heteromeric ASIC2a + 3 current

ASIC2a has been shown to be mainly expressed in medium- and large-diameter sensory neurons (Garcia-Anoveros *et al*, 2001; Alvarez de la Rosa *et al*, 2002) and has not been shown to be involved in nociceptor function. However, its contribution to native currents cannot be excluded as low ASIC2a levels have been detected in rat sensory neurons (Voilley *et al*, 2001; Alvarez de la Rosa *et al*, 2002). The ASIC2a + 3 current recorded in transfected COS cells shows a typical biphasic current with a transient phase, followed by a plateau (Babinski *et al*, 2000; Baron *et al*, 2001). APETx2 (3 μM) blocked neither the rapid nor the slow component of the ASIC2a + 3 current (not shown, $n = 5$).

Effects of APETx2 on K^+ channels

Due to its sequence homology with the BDS toxins and APETx1, APETx2 was tested on various heterologously expressed Kv channels. None of them (Kv1.4, HERG, Kv2.2, Kv3.1, Kv4.1, Kv4.2, Kv4.3) was significantly inhibited by

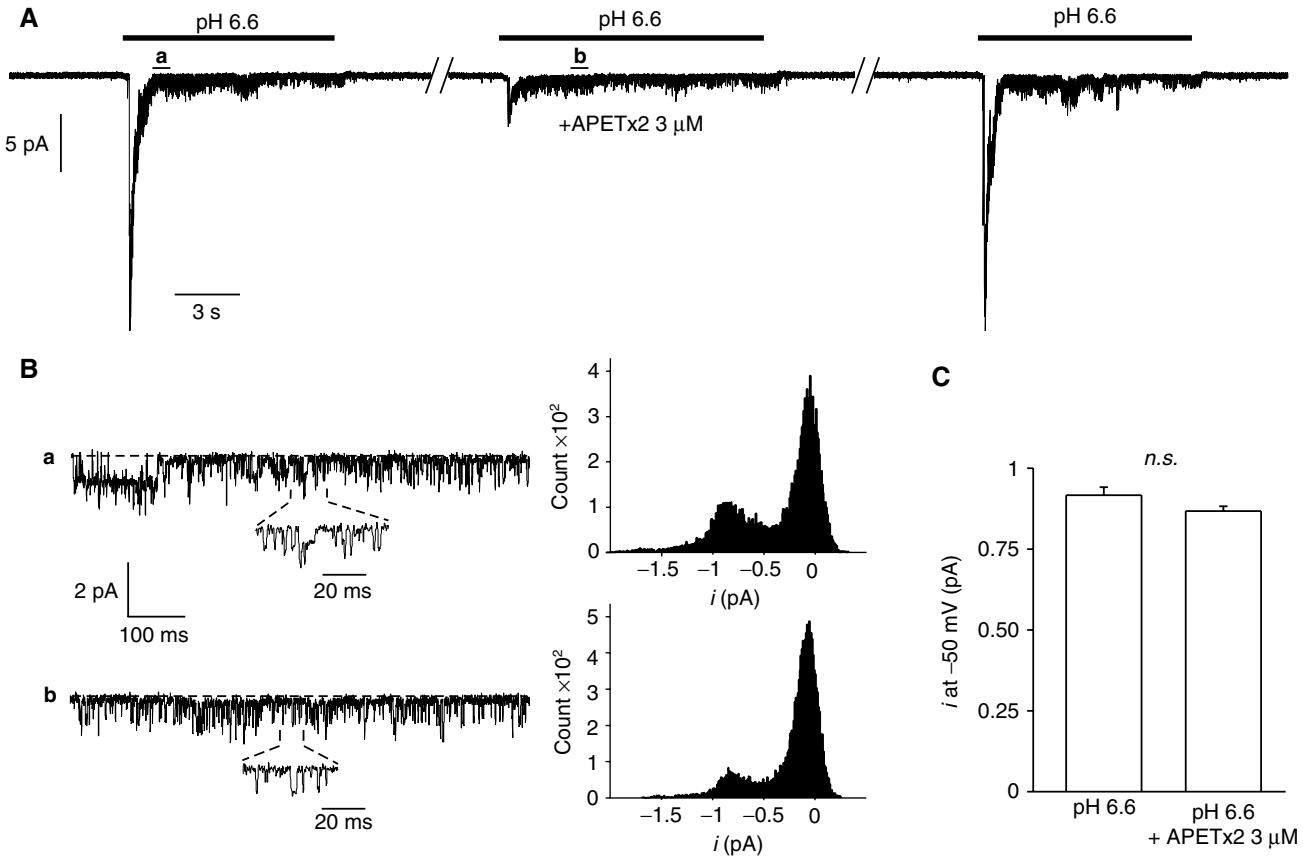

Figure 4 Effect of APETx2 on unitary ASIC3 currents recorded from outside-out patches. ASIC3 currents were recorded from COS transfected cells. Holding potential: −50 mV, pH drop from 7.4 to 6.6. (**A**) Inhibitory effect of APETx2 (3 μM) on an ASIC3 current recorded from a single excised patch. The current was triggered every minute, and APETx2 was externally applied 30 s before the second pH drop. The inhibition of ASIC3 current was 75±6% ($n=4$), and reversible. (**B**) Time-scale magnifications of parts of current trace shown in (A) (see a and b), and amplitude histograms of unitary current recorded before (a) and after (b) the application of APETx2. (**C**) Statistical analysis of ASIC3 unitary current amplitude measured at −50 mV in the presence and in the absence of APETx2 (4 excised patches, *n.s.*, nonsignificant).

300 nM APETx2. Only the Kv3.4 current was partially inhibited by much higher concentrations (3 μM) of APETx2 (38±2%, $n=6$, not shown).

APETx2 inhibits ASIC3-like currents in primary cultures of rat sensory neurons

ASIC3-like currents were selected for their lack of sensitivity (less than 20% inhibition) to PcTx1 (Escoubas *et al*, 2000a), and for their typical kinetics and pH dependency (Mamet *et al*, 2002). Among the DRG neurons recorded, 26.5% expressed a PcTx1-resistant ASIC3-like current. This biphasic current could show either a Na^+-specific current as expected for homomeric ASIC3 channels, or a nonspecific sustained cation current, probably flowing through heteromeric ASIC2b+3 channels (Lingueglia *et al*, 1997) (Figure 6A). Neurons expressing a 10 μM capsaicin-activated VR1 current were excluded. As shown by current traces in Figure 6B, APETx2 inhibited the ASIC3-like current of sensory neurons in a concentration-dependent manner when applied before the pH drop. However, the current was not fully inhibited by the toxin and 3 μM APETx2 reduced the ASIC3-like current amplitude to 51±3% ($n=11$) of the control. The sigmoidal fit of the concentration-dependent inhibition of the ASIC3-like current by APETx2 shows an IC_{50} of 219 nM (Figure 6C). A mean IC_{50} of 216±49 nM ($n=6$) was calculated from IC_{50} values obtained from six different neurons. The effect of APETx2 was the same whether the ASIC3-like current was activated at pH 6.3 or pH 5 (not shown).

Experiments have been performed on ASIC-like current recorded from sensory neurons of ASIC3 knockout adult mice (52 neurons, two primary cultures). These neurons do not express ASIC3-like current. No ASIC2-like current was recorded, consistent with previous observations that ASIC2a is essentially not expressed in DRG neurons (Lingueglia *et al*, 1997; Mamet *et al*, 2002). In 15% of recorded $ASIC3^{-}/^{-}$ DRG neurons, an ASIC1-like current was recorded, which was blocked by the ASIC1a-specific toxin PcTx1 (10 nM), but resistant to APETx2 (3 μM). This result is in agreement with the absence of inhibition of the recombinant ASIC1a current by APETx2.

APETx2 shares about 40% sequence homology with the *Anthopleura* sp. toxins, which are potent activators of voltage-dependent Na^+ channels (Romey *et al*, 1976; Kodama *et al*, 1981; Schweitz *et al*, 1981; Reimer *et al*, 1985). Therefore, we tested the effect of APETx2 on action potential triggering in sensory neurons. Figure 6D shows membrane potential variations induced by two current pulses, one infraliminar and the other reaching the action potential threshold, in the absence (top) and presence of 1 μM APETx2 (bottom) on the same neuron. APETx2 did not

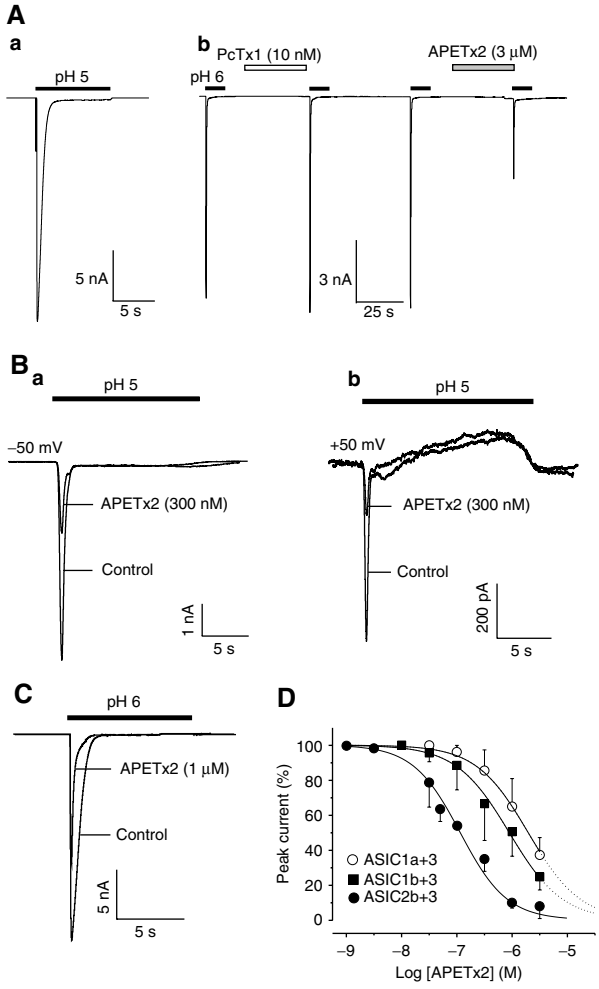

Figure 5 Effect of APETx2 on heteromeric ASIC1a + 3, ASIC1b + 3, and ASIC2b + 3 channels. ASIC subunits were co-expressed in COS cells. Drugs were perfused for 30 s before the pH drop, as indicated above each current trace. (**A**) ASIC1a + 3 current stimulated at pH 5 exhibits a peak and a plateau phase (a). At pH 6, the current is insensitive to PcTx1 (10 nM), whereas partly inhibited by APETx2 (3 μM) (b). (**B**) The peak ASIC2b + 3 current is inhibited by 300 nM of APETx2 (a) (HP = −50 mV). At + 50 mV, the peak ASIC2b + 3 current was also inhibited by the toxin (b), whereas the outward sustained phase was insensitive to APETx2 (300 nM). (**C**) The heteromeric ASIC1b + 3 current was half-inhibited by 1 μM APETx2 (HP = −50 mV). (**D**) Concentration–response relationship for APETx2 block of ASIC2b + 3 (●), ASIC1b + 3 (■), and ASIC1a + 3 (○) currents. The concentration–response curve was fitted by the Hill equation. The IC_{50} values are 117 nM, 0.9 μM, and 2 μM (n_H of 1, 0.9, and 0.9) for ASIC2b + 3, ASIC1b + 3, and ASIC1a + 3, respectively. Each point is the mean ± s.e.m. of data from three to eight cells.

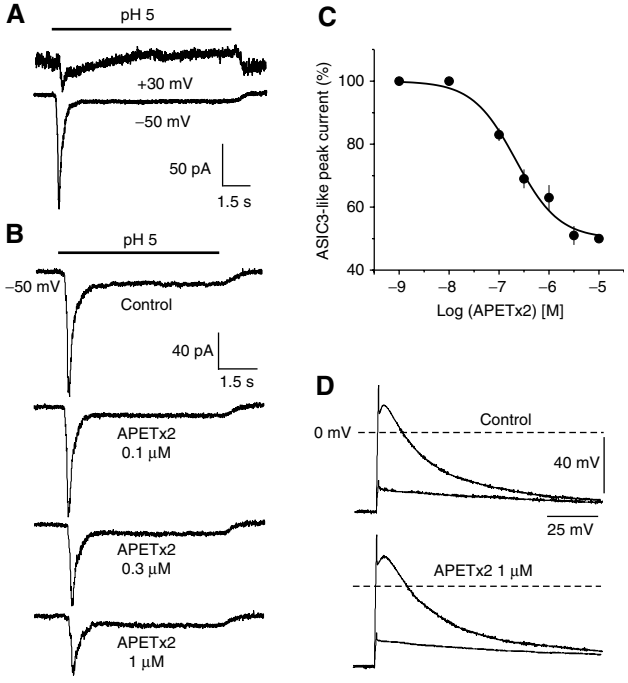

Figure 6 Effect of APETx2 on ASIC3-like current in primary cultures of rat sensory neurons. (**A**) Original current traces of an ASIC2b + 3-like current showing typical ASIC3-like kinetics at the holding potential of −50 mV and an outward sustained cation current at + 30 mV. (**B**) Original current traces of ASIC3-like current in the absence (control) and in the presence of increasing concentrations of APETx2 applied before the pH drop. This neuron expressed no VR1 current and the ASIC3-like current showed a cation nonselective plateau phase (outward current at + 30 mV, not shown). In this neuron, the ASIC3-like current was maximally inhibited by 1–3 μM APETx2 to 47% of the control amplitude, and the fit of the concentration-dependent block showed an IC_{50} = 203 nM. (**C**) Concentration–response curve of APETx2 inhibition of ASIC3-like current. The amplitude of the current in the presence of toxin was expressed as a percentage of the amplitude of control current and plotted as a function of toxin concentration. Each point is the mean ± s.e.m. of data from 5–17 cells. IC_{50} = 219 nM, n_H = 1. (**D**) Current-clamp recordings of membrane potential variations induced by the same current pulses in control (top) and in the presence of 1 μM APETx2 (bottom) on the same neuron. Two potential traces are shown under each condition: one induced by an infraliminar current pulse and the other induced by a supraliminar current pulse inducing an action potential firing. APETx2 does not significantly modify action potential triggering or kinetics.

significantly modify the action potential triggering or its kinetics, eliminating the possible nonspecific effects on voltage-dependent Na^+ and K^+ channels involved in the action potential of sensory neurons.

In vivo central injections of APETx2

Central injections of APETx2 in mice were administered to evaluate the toxicity and/or possible behavioral changes. Intracisternal injections of 5, 10, and 20 μg of APETx2 did not induce neurotoxic symptoms in mice even after 24 h. The behavior of injected mice was identical to that of control mice injected with physiological solution.

Discussion

Animal venoms have provided a great variety of toxins, which have been successfully used as tools to characterize ion channels. The emergence of specific pharmacological tools for ASIC channels started with the discovery of Psalmotoxin 1 (PcTx1), a tarantula peptide that blocks with high specificity and affinity homomeric ASIC1a channels (Escoubas *et al*, 2000a, 2003). We have now isolated and characterized APETx2, the first toxin able to inhibit selectively ASIC3-containing channels and ASIC3-like currents in DRG neurons.

APETx2 reversibly inhibited the rat ASIC3 peak current with an $IC_{50} = 63$ nM, as well as the human ASIC3 peak current with an $IC_{50} = 175$ nM. Outside-out patch recording demonstrated that APETx2 directly inhibits the ASIC3 channel, without any change in its unitary conductance. APETx2 also inhibits the heteromeric ASIC2b + 3 channel with an IC_{50} of 117 nM and heteromeric ASIC1a + 3 and ASIC1b + 3 channels with lower affinities ($IC_{50} = 2$ and 0.9 μM, respectively).

Similar to amiloride, which has been shown to inhibit ASIC3 with an $IC_{50} = 63$ μM (Waldmann *et al*, 1997a), APETx2 blocks the peak ASIC3 current without affecting the sustained plateau. Analysis of structure–function relationships of the FaNaC channel, another member of the ENaC/ASIC family (Lingueglia *et al*, 1995), has previously shown that amiloride blocks the channel by entering into the pore structure (Poet *et al*, 2001).

Although APETx2 has sequence homologies with the *Anthopleura* sp. toxins (AP-A, AP-B, AP-C), which are potent activators of voltage-dependent Na^+ channels (Romey *et al*, 1976; Kodama *et al*, 1981; Schweitz *et al*, 1981; Reimer *et al*, 1985), it does not modify the triggering or kinetics of the action potential in rat sensory neurons, thus showing no nonspecific effect on voltage-dependent Na^+ channels. This is not surprising as APETx2 was purified from a sea anemone peptide fraction devoid of paralytic activity (Bruhn *et al*, 2001). APETx2 was also non-toxic to mice after i.c. injection using doses 100–1000-fold higher than the known LD_{50} for AP-A (AxI) or AP-B (AxII) administered under the same conditions (Schweitz, 1984). Furthermore, the basic residues (Arg 12, Arg14, Lys 48, or Lys49 in AP-A or AP-B), which have been implicated in the toxin interaction with Na_v channels (Barhanin *et al*, 1981; Gallagher and Blumenthal, 1994; Khera and Blumenthal, 1994; Loret *et al*, 1994), are absent in the APETx2 primary sequence. Similarly, hydrophobic (Trp 33 in AP-B) or acidic residues (Asp7, Asp9 in AP-B), also implicated in toxin binding to the Na_v channel (Dias-Kadambi *et al*, 1996; Khera and Blumenthal, 1996), are absent in APETx2.

The structure of APETx2 is more closely related to that of the K^+ channel modulators BDS-I, BDS-II, and APETx1, purified, respectively, from *Anemonia sulcata* and *Anthopleura elegantissima* (Driscoll *et al*, 1989a, b; Diochot *et al*, 1998, 2003). These short polypeptides are folded into three-stranded antiparallel β-sheets connected by three disulfide bonds whose location is similar to that of the long sea anemone Na_v toxins (Norton, 1991; Loret *et al*, 1994). Although APETx2 shares 57, 55, and 76% sequence homologies with BDS-I, BDS-II, and APETx1, and has the same structural fold, its biological target is different. BDS-I and BDS-II are specific inhibitors of Kv3.4 channels, while APETx1 is a specific blocker of HERG K^+ channels. Despite sequence homology with APETx1, the inhibitory effect of APETx2 appears to be specific for ASIC3-containing channels. Toxin structure comparison reveals a highly conserved three-dimensional scaffold, and also two toxin areas that are significantly altered by amino-acid substitutions, probably leading to the different pharmacological profiles. As previously observed for other animal toxins, a similar scaffold is used as a basis for 'combinatorial chemistry', and slight alterations of toxin structure guide the selectivity toward different cellular receptors.

In vivo, ASIC-like currents are the result of both homomeric and heteromeric associations of ASIC subunits (Bassilana *et al*, 1997; Babinski *et al*, 2000; Alvarez de la Rosa *et al*, 2002). In order to determine their respective contribution, tools are required that block heteromeric as well as homomeric channels. To this end, APETx2 is the first toxin known to inhibit homomeric ASIC3 channels in addition to several ASIC3-containing heteromers, and thus represents a major pharmacological step in dissecting the molecular basis of acid-induced currents in sensory neurons.

ASIC1a, ASIC1b, ASIC2b, and ASIC3 are often co-expressed in sensory neurons (Lingueglia *et al*, 1997; Waldmann and Lazdunski, 1998; Alvarez de la Rosa *et al*, 2002; Mamet *et al*, 2002), and the inhibition of ASIC3-like current by APETx2 could result from a combination of the various effects of APETx2 on the different ASIC3-containing channels. The existence of ASIC2b + 3 channels is identified by the nonspecific sustained cation current that can often be recorded following the transient ASIC3-like peak (Figure 6A). ASIC1a + 3 and ASIC1b + 3 channels could also participate in the ASIC3-like current, because their electrophysiological properties (activation and inactivation kinetics, plateau phase) cannot distinguish them from the ASIC3 homomeric channel. The presence of ASIC2a + 3 channels is also possible as ASIC2a has now been identified in rat sensory neurons (Voilley *et al*, 2001; Alvarez de la Rosa *et al*, 2002), but the participation of homomeric ASIC2a channels can be ruled out in these experiments due to the low pH sensitivity of these channels ($pH_{0.5} = 4.4$, (Lingueglia *et al*, 1997; Baron *et al*, 2001)). As neurons expressing capsaicin-sensitive VR1 current were excluded and homomeric ASIC1a current were blocked by PcTx1, the partial inhibitory effect of APETx2 on ASIC3-like current in sensory neurons could then result from an inhibition of ASIC3 and ASIC2b + 3 channels, in addition to a very partial inhibition of ASIC1a + 3 and ASIC1b + 3 channels.

The discovery of a toxin with ASIC3-blocking activity is of major significance given the substantial amount of evidence now implicating this channel in the transduction of acid-induced pain and hyperalgesia. ASIC3 channel activity is dramatically increased in the presence of lactate (produced under ischemic conditions), and is responsible for sensing and transmitting pain associated with myocardial ischemia (Immke and McCleskey, 2001). ASIC channel expression, particularly ASIC3, is upregulated by proinflammatory mediators including NGF, and has been implicated in sensory neuron hyperexcitability and hyperalgesia (Mamet *et al*, 2002, 2003). In addition, ASIC3 and ASIC3-like currents are potentiated by neuropeptides that are overexpressed under inflammatory conditions (Deval *et al*, 2003).

Two independent groups reported that ASIC3 channels play a role in the modulation of pain sensation (Price *et al*, 2001; Chen *et al*, 2002), and it was recently shown that ASIC3, but not ASIC1, is involved in the development of acid-induced mechanical hyperalgesia in skeletal muscle and central sensitization (Sluka *et al*, 2003). This finding is important for understanding the development of chronic musculoskeletal pain syndromes, and identifies ASIC3 as a potential therapeutic target for treatment or prevention of chronic hyperalgesia. In addition to studies in rat and mouse models, ASIC channels have been shown to be the primary acid sensors in human nociceptors *in vivo* (Ugawa *et al*,

2002). APETx2 is the first and so far the unique peptide toxin inhibitor of ASIC3-containing channels. Along with PcTx1, APETx2 will be an important component of the pharmacological toolbox needed to determine the physiological involvement of ASIC channels in neuronal excitability and pain coding.

Materials and methods

Purification of APETx2 from Anthopleura elegantissima

A pool of polypeptides was isolated from a crude water–methanol extract of the sea anemone *Anthopleura elegantissima* (Bruhn *et al*, 2001) by anion exchange chromatography on QAE Sephadex A-25 (4.5×400 mm) eluted with ammonium acetate (pH8.3), followed by gel filtration on Sephadex G50 (12×140 cm) in acetic acid 1 M. Six fractions were tested on ASIC3 channels expressed in *Xenopus* oocytes. One fraction, which inhibited 90% of the ASIC3 current, was further purified by reversed-phase HPLC (Waters Symmetry C18, 4.6×250 mm), with a linear gradient from 10 to 40% of solvent B (10% acetonitrile/TFA 0.1%) in 30 min, at 1 ml/min. The separation was carried out on a HP1100 system (Hewlett Packard, USA) coupled to a diode-array detector with UV absorbance monitoring at 220 and 280 nm. The active fraction was then purified on a TSK-SP5PW (7.5×75 mm) cation exchange column (Tosoh, Japan) equilibrated in water/acetic acid 1% using a linear gradient from 0 to 100% ammonium acetate 1 M in 50 min at 1 ml/min. Final purification of APETx2 was carried out on the same reversed-phase HPLC column, using a linear gradient from 20 to 30% in 10 min, followed by 30–40% solvent B in 20 min.

Peptide sequencing and mass determination

APETx2 was reduced with 2-mercaptoethanol and alkylated with 4-vinylpyridine prior to N-terminal automated Edman sequencing (477A, Applied Biosystems, USA). The C-terminal sequence of the peptide was confirmed by citraconylation of the arginine residues, followed by trypsin digestion. Tryptic fragments were separated by HPLC (Waters C18, 2×150 mm) using a 40 min linear gradient from 5 to 50% of acetonitrile/TFA 0.1% in water/TFA 0.1% at 200 µl/min. Sequence homologies were determined from a BLAST search (http://www.ncbi.nlm.nih.gov/BLAST/). Molecular mass determination was carried out by MALDI-TOF Mass Spectrometry on a Voyager DE-PRO system (Applied Biosystems, USA) in reflector mode, with α-cyano-4-hydroxycinnamic acid matrix (Sigma-Aldrich, USA) and internal calibration. Mass spectra were analyzed with Data Explorer software, and theoretical molecular masses were calculated from sequence data using GPMAW (http://welcome.to/gpmaw/).

Disulfide bridge determination

The disulfide bond arrangement of APETx2 was determined using the partial reduction and cyanylation-induced cleavage method (Wu *et al*, 1996; Qi *et al*, 2001). Briefly, 5 nmol of toxin was dissolved in 5 µl of citrate buffer (0.1 M, pH 3, 6 M guanidine HCl). Partial reduction was carried out by adding 150 nmol of tris(2carboxyethyl)-phosphine hydrochloride (TCEP) and incubating for 20 min at 40°C. Cyanylation was achieved by adding a large excess (4000 nmol, pH 3) of 1-cyano-4-(dimethylamino)pyridinium tetrafluoroborate (CDAP) and incubating for 15 min at room temperature. The mixture was diluted to 200 µl with water/0.1% TFA and separated by reversed-phase HPLC using a linear gradient of 20–40% acetonitrile in water/TFA 0.1% over 40 min (Merck Purospher STAR C18 55×4.6 mm, 3 µm). After analysis by MALDI-TOF mass spectrometry, fractions containing singly and doubly reduced isoforms were vacuum-dried and dissolved in 2 µl of 1 M NH_4OH (pH 8, 6 M guanidine HCl), to which was added another 8 µl of 1 M NH_4OH for cleavage (1 h, room temperature). The NH_4OH was removed under vacuum before complete reduction with 2 µl of 0.1 M TCEP (200 nmol, citrate buffer, pH 3) for 30 min at 37°C. Samples were desalted on reversed-phase microcolumns (ZipTips C18, Millipore, USA) prior to MALDI-TOF MS analysis.

Molecular modeling

A model of APETx2 was calculated from the previously described coordinates of APETx1 (Diochot *et al*, 2003), using the DeepView Swiss-PDB viewer software v3.7 (http://us.expasy.org/spdbv/). The model was optimized via the Swiss-Model server (http://swissmodel.expasy.org/). BDS-I coordinates (1BDS) were obtained from the PDB database (http://www.rcsb.org/pdb/).

Xenopus oocytes preparation, cRNA injections, and electrophysiological measurements

Oocytes preparation and cRNA injections have been previously described (Diochot *et al*, 1998) (see online Supplementary data). Rat ASIC3 cRNA was synthesized with the mCAP RNA capping kit (Stratagene). A rapid perfusion system allowed local and rapid changes of extracellular solutions. Depending on the pH range, solutions were buffered with HEPES (pH > 6), MES (pH between 6 and 5) or acetate (pH < 5).

COS cell transfections

COS-7 cells were transfected with pCI-rASIC1a, pCI-rASIC1b, pCI-rASIC2a, pCI-rASIC2b, pCI-rASIC3, and pCI-hASIC3 as previously described (Lingueglia *et al*, 1997; Anzai *et al*, 2002). For heteromeric expression, cells were co-transfected with pCI-rASIC2a and pCI-rASIC3 (1:1 ratio) or pCI-rASIC2b and pCI-rASIC3 (1:1 ratio), and with an expression vector containing the CD8 receptor cDNA, using the DEAE-dextran method. The heteromeric expressions of ASIC1a + 3 and ASIC1b + 3 were achieved using the pBudCE4.1 vector (Invitrogen), which contains the human cytomegalovirus (CMV) immediate-early promoter and the human elongation factor 1α-subunit (EF-1α) promoter for high-level, constitutive, independent expression of two recombinant proteins. Rat ASIC3 (Accession Number # AAB69328) was subcloned under the control of the EF-1α promoter, whereas rat ASIC1a (Accession Number # U94403) or rat ASIC1b (Accession Number # AJ309926) was subcloned under the control of the CMV promoter. K^+ channels were expressed using 0.01 µg of pCI-rKv1.4, pCI-rKv2.2, pRc/CMV rKv3.4, 0.05 µg of pCI-rKv4.1, pCI-rKv4.2, pCI-rKv4.3, and pSI-rHERG per dish. Currents in COS-7 cells were recorded at room temperature (22°C) within 1–2 days of transfection.

Primary culture of sensory neurons

Dorsal root ganglia were dissected from Wistar rats (5–7 weeks) and enzymatically dissociated with 0.1% collagenase. Cells were then plated on collagen-coated 35 mm Petri dishes and maintained in culture at 37°C (95% air/5% CO_2) in DMEM containing 5% fetal calf serum. Electrophysiological experiments were carried out 1 or 2 days after plating (Mamet *et al*, 2002).

Patch-clamp recording

Currents were sampled at 3.3 or at 20 kHz for whole-cell and outside-out patch-clamp recordings (Hamill *et al*, 1981), and low-pass filtered at 3 kHz using pClamp8 software (Axon Instruments). Off-line analysis of currents was performed using pClamp and BioPatch (Bio-Logic Science Instruments). The pipette solution contained (in mM): KCl 140, NaCl 5, $MgCl_2$ 2, EGTA 5, HEPES-KOH 10 (pH 7.4) and the bath solution contained (in mM): NaCl 140, KCl 5, $MgCl_2$ 2, $CaCl_2$ 2, BSA 0.1%, HEPES-NaOH 10 (pH 7.4). Depending on the pH range, solutions were buffered with HEPES (pH > 6), MES (pH between 6 and 5) or acetate (pH < 5). Solutions were applied locally by a rapid perfusion system. For experiments with sensory neurons, glucose 10 mM, CNQX 20 µM, and kynurenic acid 10 µM (to inhibit glutamate-activated ionotropic currents) were added to the bath solution, and the pipette solution contained (in mM): KCl 140, ATP-Na_2 2.5, $MgCl_2$ 2, $CaCl_2$ 2, EGTA 5, and HEPES 10 (pH 7.3, pCa estimated to 7).

Analysis

Concentration–response curves were fitted by the Hill equation:

$$I = \mathrm{Imax} + (\mathrm{Imin} - \mathrm{Imax})(C^{n_H}/(C^{n_H} + \mathrm{IC}_{50}^{n_H}))$$

where I is the amplitude of relative current, Imax is the maximum current amplitude, Imin is the minimum current amplitude, C is the toxin concentration, IC_{50} is the toxin concentration that half-maximally inhibited the current, and n_H is the Hill coefficient. The results are expressed as mean ± standard error of the mean (s.e.m.). Statistical significance was determined using the Student's t-test ($P < 0.05$*, $P < 0.01$**, $P < 0.005$***).

Mouse intracisternal injections

Anesthetized 5-week-old outbred OF1 (Charles River) mice were injected intracisternally with 1–5 µl APETx2 diluted in sterile NaCl solution (0.9% NaCl, 0.1% BSA). Symptoms were observed during the first hour after injection and at regular intervals over 24 h. Control mice were injected with 5 µl of NaCl solution.

Supplementary data

Supplementary data are available at *The EMBO Journal* Online.

Acknowledgements

We thank D Moinier, M Jodar, and V Briet for technical assistance, and Dr L Beress for generously and kindly providing sea anemone extracts. This work was supported by the Centre National de la Recherche Scientifique (CNRS), the Ministère de la Recherche et de la Technologie, the Association pour la Recherche contre le Cancer (ARC), Astra Zeneca AB Research Area CNS/Pain, and the Association Française contre les Myopathies (AFM). LD Rash is supported by an INSERM/NH&MRC fellowship (ID 194470).

References

Akopian AN, Chen CC, Ding Y, Cesare P, Wood JN (2000) A new member of the acid-sensing ion channel family. *Neuroreport* **11:** 2217–2222

Alvarez de la Rosa D, Zhang P, Shao D, White F, Canessa CM (2002) Functional implications of the localization and activity of acid-sensitive channels in rat peripheral nervous system. *Proc Natl Acad Sci USA* **99:** 2326–2331

Anzai N, Deval E, Schaefer L, Friend V, Lazdunski M, Lingueglia E (2002) The multivalent PDZ domain-containing protein CIPP is a partner of acid-sensing ion channel 3 in sensory neurons. *J Biol Chem* **277:** 16655–16661

Askwith CC, Cheng C, Ikuma M, Benson C, Price MP, Welsh MJ (2000) Neuropeptide FF and FMRFamide potentiate acid-evoked currents from sensory neurons and proton-gated DEG/ENaC channels. *Neuron* **26:** 133–141

Babinski K, Catarsi S, Biagini G, Seguela P (2000) Mammalian ASIC2a and ASIC3 subunits co-assemble into heteromeric proton-gated channels sensitive to Gd3+. *J Biol Chem* **275:** 28519–28525

Babinski K, Le KT, Seguela P (1999) Molecular cloning and regional distribution of a human proton receptor subunit with biphasic functional properties. *J Neurochem* **72:** 51–57

Barhanin J, Hugues M, Schweitz H, Vincent JP, Lazdunski M (1981) Structure–function relationships of sea anemone toxin II from *Anemonia sulcata*. *J Biol Chem* **256:** 5764–5769

Baron A, Schaefer L, Lingueglia E, Champigny G, Lazdunski M (2001) Zn^{2+} and H^+ are coactivators of acid-sensing ion channels. *J Biol Chem* **276:** 35361–35367

Bassilana F, Champigny G, Waldmann R, de Weille JR, Heurteaux C, Lazdunski M (1997) The acid-sensitive ionic channel subunit ASIC and the mammalian degenerin MDEG form a heteromultimeric H^+-gated Na^+ channel with novel properties. *J Biol Chem* **272:** 28819–28822

Benson CJ, Eckert SP, McCleskey EW (1999) Acid-evoked currents in cardiac sensory neurons: a possible mediator of myocardial ischemic sensation. *Circ Res* **84:** 921–928

Bode F, Sachs F, Franz MR (2001) Tarantula peptide inhibits atrial fibrillation. *Nature* **409:** 35–36

Bruhn T, Schaller C, Schulze C, Sanchez-Rodriguez J, Dannmeier C, Ravens U, Heubach JF, Eckhardt K, Schmidtmayer J, Schmidt H, Aneiros A, Wachter E, Beress L (2001) Isolation and characterisation of five neurotoxic and cardiotoxic polypeptides from the sea anemone *Anthopleura elegantissima*. *Toxicon* **39:** 693–702

Chen CC, England S, Akopian AN, Wood JN (1998) A sensory neuron-specific, proton-gated ion channel. *Proc Natl Acad Sci USA* **95:** 10240–10245

Chen CC, Zimmer A, Sun WH, Hall J, Brownstein MJ (2002) A role for ASIC3 in the modulation of high-intensity pain stimuli. *Proc Natl Acad Sci USA* **99:** 8992–8997

Coscoy S, de Weille JR, Lingueglia E, Lazdunski M (1999) The pretransmembrane 1 domain of acid-sensing ion channels participates in the ion pore. *J Biol Chem* **274:** 10129–10132

de Weille JR, Bassilana F, Lazdunski M, Waldmann R (1998) Identification, functional expression and chromosomal localisation of a sustained human proton-gated cation channel. *FEBS Lett* **433:** 257–260

Deval E, Baron A, Lingueglia E, Mazarguil H, Zajac JM, Lazdunski M (2003) Effects of neuropeptide SF and related peptides on acid sensing ion channel 3 and sensory neuron excitability. *Neuropharmacology* **44:** 662–671

Dias-Kadambi BL, Combs KA, Drum CL, Hanck DA, Blumenthal KM (1996) The role of exposed tryptophan residues in the activity of the cardiotonic polypeptide anthopleurin B. *J Biol Chem* **271:** 23828–23835

Diochot S, Loret E, Bruhn T, Beress L, Lazdunski M (2003) APETx1, a new toxin from the sea anemone *Anthopleura elegantissima*, blocks voltage-gated human ether-a-go-go-related gene potassium channels. *Mol Pharmacol* **64:** 59–69

Diochot S, Schweitz H, Beress L, Lazdunski M (1998) Sea anemone peptides with a specific blocking activity against the fast inactivating potassium channel Kv3.4. *J Biol Chem* **273:** 6744–6749

Driscoll PC, Clore GM, Beress L, Gronenborn AM (1989a) A proton nuclear magnetic resonance study of the antihypertensive and antiviral protein BDS-I from the sea anemone *Anemonia sulcata*: sequential and stereospecific resonance assignment and secondary structure. *Biochemistry* **28:** 2178–2187

Driscoll PC, Gronenborn AM, Beress L, Clore GM (1989b) Determination of the three-dimensional solution structure of the antihypertensive and antiviral protein BDS-I from the sea anemone *Anemonia sulcata*: a study using nuclear magnetic resonance and hybrid distance geometry-dynamical simulated annealing. *Biochemistry* **28:** 2188–2198

England LJ, Imperial J, Jacobsen R, Craig AG, Gulyas J, Akhtar M, Rivier J, Julius D, Olivera BM (1998) Inactivation of a serotonin-gated ion channel by a polypeptide toxin from marine snails. *Science* **281:** 575–578

Escoubas P, Bernard C, Lambeau G, Lazdunski M, Darbon H (2003) Recombinant production and solution structure of PcTx1, the specific peptide inhibitor of ASIC1a proton-gated cation channels. *Protein Sci* **12:** 1332–1343

Escoubas P, De Weille JR, Lecoq A, Diochot S, Waldmann R, Champigny G, Moinier D, Menez A, Lazdunski M (2000a) Isolation of a tarantula toxin specific for a class of proton-gated Na^+ channels. *J Biol Chem* **275:** 25116–25121

Escoubas P, Diochot S, Corzo G (2000b) Structure and pharmacology of spider venom neurotoxins. *Biochimie* **82:** 893–907

Gallagher MJ, Blumenthal KM (1994) Importance of the unique cationic residues arginine 12 and lysine 49 in the activity of the cardiotonic polypeptide anthopleurin B. *J Biol Chem* **269:** 254–259

Garcia-Anoveros J, Samad TA, Zuvela-Jelaska L, Woolf CJ, Corey DP (2001) Transport and localization of the DEG/ENaC ion channel BNaC1alpha to peripheral mechanosensory terminals of dorsal root ganglia neurons. *J Neurosci* **21:** 2678–2686

Grunder S, Geissler HS, Bassler EL, Ruppersberg JP (2000) A new member of acid-sensing ion channels from pituitary gland. *Neuroreport* **11:** 1607–1611

Hamill OP, Marty A, Neher E, Sakmann B, Sigworth FJ (1981) Improved patch-clamp techniques for high-resolution current recording from cells and cell-free membrane patches. *Pflugers Arch* **391:** 85–100

Harvey AL, Rowan EG, Vatanpour H, Fatehi M, Castaneda O, Karlsson E (1994) Potassium channel toxins and transmitter release. *Ann NY Acad Sci* **710:** 1–10

Hugues M, Romey G, Duval D, Vincent JP, Lazdunski M (1982) Apamin as a selective blocker of the calcium-dependent potassium channel in neuroblastoma cells: voltage-clamp and biochemical characterization of the toxin receptor. *Proc Natl Acad Sci USA* **79:** 1308–1312

Immke DC, McCleskey EW (2001) Lactate enhances the acid-sensing Na^+ channel on ischemia-sensing neurons. *Nat Neurosci* **4:** 869–870

Khera PK, Blumenthal KM (1994) Role of the cationic residues arginine 14 and lysine 48 in the function of the cardiotonic polypeptide anthopleurin B. *J Biol Chem* **269:** 921–925

Khera PK, Blumenthal KM (1996) Importance of highly conserved anionic residues and electrostatic interactions in the activity and structure of the cardiotonic polypeptide anthopleurin B. *Biochemistry* **35:** 3503–3507

Kodama I, Shibata S, Toyama J, Yamada K (1981) Electromechanical effects of anthopleurin-A (AP-A) on rabbit ventricular muscle: influence of driving frequency, calcium antagonists, tetrodotoxin, lidocaine and ryanodine. *Br J Pharmacol* **74:** 29–37

Kress M, Zeilhofer HU (1999) Capsaicin, protons and heat: new excitement about nociceptors. *Trends Pharmacol Sci* **20:** 112–118

Krishtal O (2003) The ASICs: signaling molecules? Modulators? *Trends Neurosci* **26:** 477–483

Lingueglia E, Champigny G, Lazdunski M, Barbry P (1995) Cloning of the amiloride-sensitive FMRFamide peptide-gated sodium channel. *Nature* **378:** 730–733

Lingueglia E, de Weille JR, Bassilana F, Heurteaux C, Sakai H, Waldmann R, Lazdunski M (1997) A modulatory subunit of acid sensing ion channels in brain and dorsal root ganglion cells. *J Biol Chem* **272:** 29778–29783

Loret EP, del Valle RM, Mansuelle P, Sampieri F, Rochat H (1994) Positively charged amino acid residues located similarly in sea anemone and scorpion toxins. *J Biol Chem* **269:** 16785–16788

Mamet J, Baron A, Lazdunski M, Voilley N (2002) Proinflammatory mediators, stimulators of sensory neuron excitability via the expression of acid-sensing ion channels. *J Neurosci* **22:** 10662–10670

Mamet J, Lazdunski M, Voilley N (2003) How NGF drives physiological and inflammatory expressions of acid-sensing Ion channel 3 in sensory neurons. *J Biol Chem* **30:** 30

Moczydlowski E, Lucchesi K, Ravindran A (1988) An emerging pharmacology of peptide toxins targeted against potassium channels. *J Membr Biol* **105:** 95–111

Norton RS (1991) Structure and structure–function relationships of sea anemone proteins that interact with the sodium channel. *Toxicon* **29:** 1051–1084

Pan HL, Longhurst JC, Eisenach JC, Chen SR (1999) Role of protons in activation of cardiac sympathetic C-fibre afferents during ischaemia in cats. *J Physiol* **518:** 857–866

Poet M, Tauc M, Lingueglia E, Cance P, Poujeol P, Lazdunski M, Counillon L (2001) Exploration of the pore structure of a peptide-gated Na^+ channel. *EMBO J* **20:** 5595–5602

Price MP, McIlwrath SL, Xie J, Cheng C, Qiao J, Tarr DE, Sluka KA, Brennan TJ, Lewin GR, Welsh MJ (2001) The DRASIC cation channel contributes to the detection of cutaneous touch and acid stimuli in mice. *Neuron* **32:** 1071–1083

Price MP, Snyder PM, Welsh MJ (1996) Cloning and expression of a novel brain Na^+ channel. *J Biol Chem* **271:** 7879–7882

Qi J, Wu J, Somkuti GA, Watson JT (2001) Determination of the disulfide structure of sillucin, a highly knotted, cysteine-rich peptide, by cyanylation/cleavage mass mapping. *Biochemistry* **40:** 4531–4538

Reeh PW, Steen KH (1996) Tissue acidosis in nociception and pain. *Prog Brain Res* **113:** 143–151

Reimer NS, Yasunobu CL, Yasunobu KT, Norton TR (1985) Amino acid sequence of the *Anthopleura xanthogrammica* heart stimulant, anthopleurin-B. *J Biol Chem* **260:** 8690–8693

Romey G, Abita JP, Schweitz H, Wunderer G, Lazdunski M (1976) Sea anemone toxin: a tool to study molecular mechanisms of nerve conduction and excitation–secretion coupling. *Proc Natl Acad Sci USA* **73:** 4053–4055

Schweitz H (1984) Lethal potency in mice of toxins from scorpion, sea anemone, snake and bee venoms following intraperitoneal and intracisternal injection. *Toxicon* **22:** 308–311

Schweitz H, Vincent JP, Barhanin J, Frelin C, Linden G, Hugues M, Lazdunski M (1981) Purification and pharmacological properties of eight sea anemone toxins from *Anemonia sulcata*, *Anthopleura xanthogrammica*, *Stoichactis giganteus*, and *Actinodendron plumosum*. *Biochemistry* **20:** 5245–5252

Shakkottai VG, Regaya I, Wulff H, Fajloun Z, Tomita H, Fathallah M, Cahalan MD, Gargus JJ, Sabatier JM, Chandy KG (2001) Design and characterization of a highly selective peptide inhibitor of the small conductance calcium-activated K^+ channel, SkCa2. *J Biol Chem* **276:** 43145–43151

Sluka KA, Price MP, Breese NM, Stucky CL, Wemmie JA, Welsh MJ (2003) Chronic hyperalgesia induced by repeated acid injections in muscle is abolished by the loss of ASIC3, but not ASIC1. *Pain* **106:** 229–239

Sutherland SP, Benson CJ, Adelman JP, McCleskey EW (2001) Acid-sensing ion channel 3 matches the acid-gated current in cardiac ischemia-sensing neurons. *Proc Natl Acad Sci USA* **98:** 711–716

Tytgat J, Chandy KG, Garcia ML, Gutman GA, Martin-Eauclaire MF, van der Walt JJ, Possani LD (1999) A unified nomenclature for short-chain peptides isolated from scorpion venoms: alpha-KTx molecular subfamilies. *Trends Pharmacol Sci* **20:** 444–447

Uchitel OD (1997) Toxins affecting calcium channels in neurons. *Toxicon* **35:** 1161–1191

Ugawa S, Ueda T, Ishida Y, Nishigaki M, Shibata Y, Shimada S (2002) Amiloride-blockable acid-sensing ion channels are leading acid sensors expressed in human nociceptors. *J Clin Invest* **110:** 1185–1190

Voilley N, de Weille J, Mamet J, Lazdunski M (2001) Nonsteroid anti-inflammatory drugs inhibit both the activity and the inflammation-induced expression of acid-sensing ion channels in nociceptors. *J Neurosci* **21:** 8026–8033

Waldmann R, Bassilana F, De Weille JR, Champigny G, Heurteaux C, Lazdunski M (1997a) Molecular cloning of a non-inactivating proton-gated Na^+ channel specific for sensory neurons. *J Biol Chem* **272:** 20975–20978

Waldmann R, Champigny G, Bassilana F, Heurteaux C, Lazdunski M (1997b) A proton-gated cation channel involved in acid-sensing. *Nature* **386:** 173–177

Waldmann R, Champigny G, Voilley N, Lauritzen I, Lazdunski M (1996) The mammalian degenerin MDEG, an amiloride-sensitive cation channel activated by mutations causing neurodegeneration in *Caenorhabditis elegans*. *J Biol Chem* **271:** 10433–10436

Waldmann R, Lazdunski M (1998) H(+)-gated cation channels: neuronal acid sensors in the NaC/DEG family of ion channels. *Curr Opin Neurobiol* **8:** 418–424

Wu J, Gage DA, Watson JT (1996) A strategy to locate cysteine residues in proteins by specific chemical cleavage followed by matrix-assisted laser desorption/ionization time-of-flight mass spectrometry. *Anal Biochem* **235:** 161–174

Xie J, Price MP, Berger AL, Welsh MJ (2002) DRASIC contributes to pH-gated currents in large dorsal root ganglion sensory neurons by forming heteromultimeric channels. *J Neurophysiol* **87:** 2835–2843